RESEARCH ON SUSTAINABLE DEVELOPMENTS FOR ENVIRONMENT MANAGEMENT

Effect of fine recycled aggregate on the strength and durability properties of concrete modified through two-stage mixing approach

Jagan Sivamani[1] · Neelakantan Thurvas Renganathan[1]

Abstract

To overcome the scarcity of river sand and dumping of construction and demolition wastes, the fine recycled aggregate (FRA) collected from C&D wastes is being utilized as a replacement to river sand. Many earlier studies reported that the higher water absorption of fine recycled aggregate and weak interfacial transition zone (ITZ) resulted in the development of the concrete with less strength and durability requirements. This study surmounts the above two factors through pre-saturation and a two-stage mixing approach (TSMA) technique. The concrete mixes prepared at 0.45 w/c ratios with 0%, 25%, 50%, and 100% of FRA were evaluated through hardened properties such as compressive strength, split tensile strength, flexural strength, and durability properties such as water absorption, sorptivity, shrinkage, rapid chloride penetration, and carbonation tests. The results indicate that the optimum level of replacement of fine recycled aggregate was 25% and the increase of fine recycled aggregate decreases the strength and durability properties. However, increased curing of concrete resulted in better strength and durability properties. The strength of the concrete was increased by 12% at 28 days and 17.46% at 90 days by two-stage mixing approach. The water absorption, porosity, shrinkage, chloride penetration, and carbonation of two-stage mixing approach was decreased by 7.45%, 15.38%, 16.57%, 18.18%, and 13.51% compared to normal mixing approach. Microstructural investigations show improvement in the interfacial transition zone with two-stage mixing approach compared to normal mixing approach.

Keywords Fine recycled aggregate · Two-stage mixing approach · Normal mixing approach · Interfacial transition zone

Introduction

Concrete is the extensively produced building material in the world. The production of concrete increases up to tonnes per capita every year in which 70% comprises aggregates. Nearly one-third of the concrete produced end up as C&D wastes that were being dumped in the landfills generating municipal solid wastes. Consequently, nearly 40 billion tons of natural resources were used as raw materials for the manufacture of concrete every year (Vivian et al. 2018) causing shortage of construction materials. This necessitated the utilization of C&D wastes as a suitable replacement to natural coarse

aggregate (NCA) in the concrete. In general, the quality of RCA was inferior compared to NCA due to the inferior quality of RCA resulting from the poor quality of parent concrete. The possible use of RCA derived from C&D wastes has established its rising importance due to its prospective to be utilized in the field of construction. Moreover, the shortage in supply of NCA has necessitated the development of RCA as an alternative resource. Despite to promote sustainability with the use of RCA, the poor quality of RCA has limited its application. Several researches on the utilization of RCA as a suitable replacement to natural coarse aggregates (NCA) have been performed to study its effect on the properties of the concrete (Katz 2004, Saravanakumar et al. 2016, Abrahams and Rakesh 2018, Liang et al. 2015, Revathi et al. 2014). The studies reported the limitation on the utilization of RCA due to the higher water absorption resulting from the presence of adhered mortar. The research on the recycling of C&D wastes has prolonged further for its replacement to natural fine aggregate (NFA) in the concrete. Few researches have been carried out investigating the extent of utilization of FRA in the concrete. Similar to RCA, the higher utilization of FRA affects the

✉ Jagan Sivamani
s.jagan@klu.ac.in

[1] Department of Civil Engineering, Kalasalingam Academy of Research and Education, Anand Nagar, Krishnankoil, Tamil Nadu 626 126, India

strength and durability properties of the concrete due to the weak ITZ ensuing from its high porosity (Ho et al. 2013; Otsuki et al. 2003; Poon et al. 2004). However, only a few studies encompass improving the ITZ of the FRA concrete (FRAC) rather than the optimization of FRA in the concrete.

Pereira et al. (2012) and Berredjem et al. (2020) infer that as the replacement of FRA increases, workability and strength of the concrete reduces, but upon addition of SP, the strength of the concrete was increased even at 100% replacement. The study reported that weakness of ITZ due to the higher porosity of FRA decreases the strength of FRAC. Kirthika and Singh (2020) observed that the increase in the replacement of the FRA decreased the strength and durability of the FRAC, but densification of micro-structure in the FRAC mixes upon increased curing improved the properties of the FRAC. Leite and Leite (2019) observed that the water absorption of FRA was 90.6% more compared to NFA and also infer that the mix with 60% of NFA and 40% of FRA shows better particle packing with less voids. The decrease in the percentage of FRA may be attributed to the less fineness modulus, dry specific density, and dry bulk density of FRA. Li et al. (2019) used FRA of size ranging from 4.75 mm–75μ and infer that as the particle size reduces the water absorption and drying shrinkage increases due to the increased water demand by the higher specific surface FRA particles. Fan et al. (2016) obtained FRA from two different sources and observed variation in the properties of the FRAC due to the rough texture and friction. Results indicate that strength of the FRAC decreases with increase in the replacement of FRA. Khoshkenari et al. (2014) used 0–2 mm FRA produced from tested reinforced concrete beams and observed that the water absorption of RCA and FRA was 11.5% and 3.5% more compared to natural aggregates. Geng and Sun (2013) used three different types of FRA and observed that concrete containing derivative of FRA obtained through the sieving of collected FRA particles shows lesser slump and improved strength and durability properties. Results of carbonation indicate that decrease in the w/c ratio increased the rate of resistance of FRAC. Braga et al. (2012) infer that increase in the w/c ratio and replacement of FRA increases the porosity of the FRAC and thus reduces the strength of the mortar. The excessive fines in the FRA absorb more water and reduce the strength of the mortar. Sim and Park (2011) observed that steam-cured FRAC shows better strength compared to water-cured FRAC irrespective of the replacement levels. Also, increased curing improved the durability properties of the FRAC as the depth of chloride ion penetration of FRAC is 15.4 mm at 28 days and only 5.8 mm at 56 days. Zega and Di Maio (2011) optimized the level of replacement of FRA as 30% and infer that water absorption and sorptivity FRAC is 15% and 13% more compared to the NAC due to the higher water absorption of FRA. Evangelista et al. (2010) used FRA from crushed concrete and observed that the water absorption and sorptivity of

FRAC was 46% and 70.3% more compared to NAC. Similarly, 33% increase in the chloride penetration and 110% increase in the carbonation of FRAC compared to NAC was observed.

Research significance

Several research works have been carried out with FRA as a suitable replacement to NFA, and it observed that the strength and durability of FRAC were affected with increase in the replacement of FRA. This is due to the weak ITZ of FRAC resulting from the higher porosity of FRA. However, fewer studies performed with pre-saturated FRA to counteract the higher water absorption do not strengthen the ITZ in the FRAC. Therefore, this study investigates on the improvement in the ITZ that enhances the properties of FRAC. In this study, the concrete mixes were prepared with 0%, 25%, 50%, and 100% of FRA by normal mixing approach (NMA) and two-stage mixing approach (TSMA) at 0.45 w/c ratios. The influence of FRA on the properties of concrete was evaluated through hardened properties such as compressive strength, split tensile strength, flexural strength, and durability properties such as water absorption, sorptivity, drying shrinkage, chloride penetration, and carbonation studies.

Experimental program

Materials

Forty-three grades Ordinary Portland Cement (OPC) tested for its properties as per IS 4031–1988 is given in the Table 1. The concrete fractions sampled from a 50-year-old

Table 1 Properties of OPC

Description	Values
Physical properties	
Setting time (initial)	27 mins
Setting time (final)	542 mins
Characteristic strength	44.28 MPa
Blaine's specific surface area	274 m^2/kg
Chemical properties	
Loss on ignition (LOI)	3.41 %
Magnesia	4.18 %
Insoluble residue	2.17 %
Sulfuric anhydride	3.12 %
Total chloride content	0.04 %
CaO - SiO$_2$ + Al$_2$O$_3$ + Fe$_2$O$_3$	0.72 %
Al$_2$O$_3$/Fe$_2$O$_3$	1.14 %

demolished building at Structural Engineering Research Center (SERC), India, were crushed through jaw crusher and sieved to a suitable size ranging from 75μ to 2.36mm. The sieved fractions were washed thoroughly with potable water to remove finer dust particles. The samples were then pre-saturated in water for 24 h and air dried under laboratory conditions for 4 h. The aggregates are weighed at each stage to determine the difference in the mass of the samples. This is performed to maintain surface saturated dry density (SSD) before mixing in the concrete wherein the surface of aggregates are dry but the internal pores are saturated with water. River sand and natural gravel were collected from the local suppliers and used as NFA and NCA in the study. The visual observation of NFA and FRA is shown in Fig. 1. From Fig. 1, it is observed that the texture of FRA was more angular and rough with cementitious particles smeared on its surface. Figure 6a indicates microstructural images of the angular and rough texture of FRA. The NCA with specific gravity of 2.54~2.71, fineness modulus of 6.71~7.13, and water absorption of 0.74~1.18% was sieved to a fractions ranging 10 mm~20 mm, respectively. Potable water with pH>7 was used for casting and curing of the concrete. Figure 2 shows the XRD and SEM images of NCA used in the study. The peaks in the XRD pattern of NCA indicate the presence of SiO_2, $NaAlSiO_3O_8$, and $CaCO_3$. The highest peak of SiO_2 indicates the crystalline nature could be favorable in the formation of C-S-H and C-A-S-H gel that influence the strength of the concrete. The SEM images of NCA show a dense, less angular with closely packed crystal particles.

Mix proportions and specimen preparation

The concrete mixes are prepared to achieve characteristic target strength of M30 grade at 28 days as per IS 10262-2009. The NFA was replaced by 25%, 50%, and 100% of RFA by its weight. The first set of concrete mix prepared with cement, NFA, and NCA as ingredients was labeled as NAC. The second set of concrete mix prepared by normal mixing approach (NMA) with different percentages of FRA, cement, NFA, and NCA was labeled as FRAC. The third set of concrete mix prepared by two-stage mixing approach (TSMA) with

different percentages of FRA, cement, NFA, and NCA was labeled as M-FRAC. The TSMA ascertain by Tam et al. (2005) was illustrated in Fig. 3. The details of mix proportions were given in Table 2. The fresh concrete mixture prepared by NMA and TSMA were evaluated by slump test with standard cone of 10 cm × 20 cm × 30 cm. The cube molds of 150 mm, cylindrical molds of 150 mm × 300 mm, and prism molds of 500 mm × 100 mm × 100 mm were fabricated to evaluate the hardened properties of the concrete at 7, 28, and 90 days. The water absorption of the concrete was performed with 150 mm cubes at 28 and 90 days. The capillary absorption was performed with 100 mm × 50 mm concrete discs at 5, 15, 30, 60, 120, 180, 240, and 300 mins, respectively. The shrinkage of the concrete mixes was determined with 500 mm × 100 mm × 100 mm prisms at 7, 28, 56, and 90 days. The chloride ion penetration test was performed with 100 mm × 50 mm concrete discs at 30 and 60 days, respectively. The carbonation test was performed with 150 mm cubes at 30, 60, and 90 days.

Testing of specimens

The workability of the fresh mixes prepared by NMA and TSMA were evaluated by slump cone test as per IS 1199-1999. The fresh concrete mixes fabricated into cubes, cylinders, and prisms were demolded after 24 h and cured at 20°C with relative humidity >80% at the respective ages. The compressive strength and split tensile strength was performed on cubes and cylinders as per ASTM C39/C39M–20. The flexural strength was performed on prisms as per ASTM C 78. Three specimens per mix were casted and tested for hardened properties at 7, 28, and 90 days to record the average value. The water absorption test was performed on cubes at 28 and 90 days as per ASTM C1585. The initial dry weight of the hardened specimens were noted and immersed in water for 28 and 90 days at 20°C with R.H>80%. The specimens were removed at the respective ages, dried, and weighed, and the difference in the weight measures the water absorption of the concrete. The capillary absorption was performed on cylindrical discs as per BS 1881-208. The specimens cured at 28 days were oven dried at 110°C. The sides of the specimens were coated with non-absorbent sealants and placed in such a way

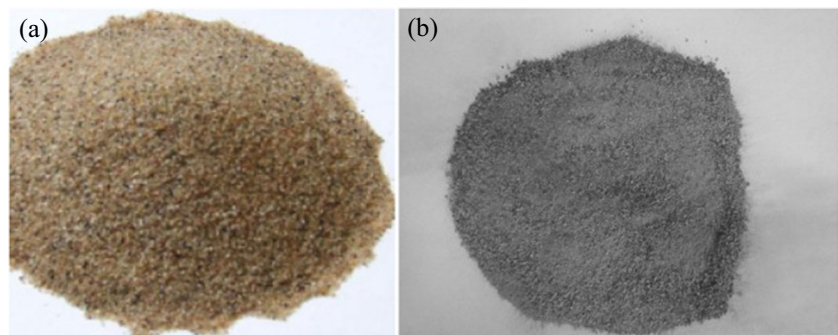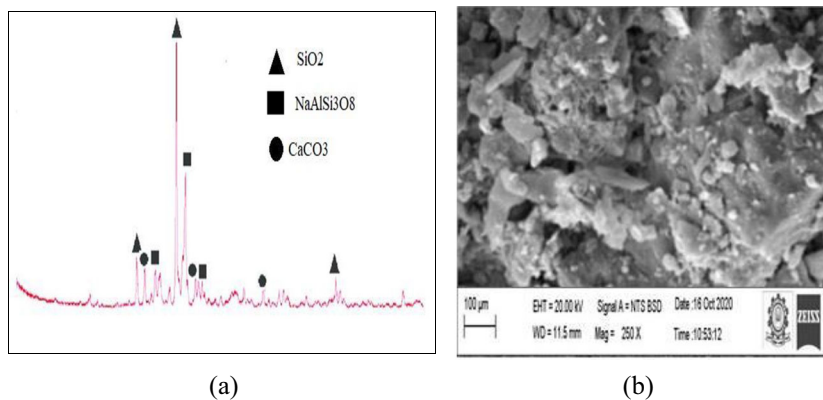**Fig. 1** Visual observation of **a** NFA and **b** FRA

Fig. 2 NCA (**a**) XRD pattern (**b**) SEM image

(a)   (b)

that water percolates through the bottom of the specimen. The rate of water uptake at intervals of 5, 15, 30, 60, 120, 180, 240, and 300 min was determined. The shrinkage was performed on 500 mm × 100 mm × 100 mm prisms as per ASTM C 596-2018. After 24 h, the initial shrinkage of the specimen was determined, and the specimens were cured in water under laboratory conditions at 25 to 30 °C for 7, 28, and 90 days. After curing at suitable ages, the specimens were removed; the surface was wiped out and was mounted on the length comparator to determine the relative difference in the length of the specimen (Kirthika and Singh 2020). The carbonation resistance of the concrete mixtures was performed at 30, 60, and 90 days (Geng and Sun 2013). The specimens were cured at 20°C and dried for 48 h at 60°C. The accelerated carbonation test was conducted with 25% of CO_2 concentration at 20 ± 5°C. The samples after carbonation were removed from the chamber, split, and sprayed with 1% of phenolphthalein indicator to determine the rate of carbonation in the concrete. The resistance of the concrete mixes to the ingression of chloride ions was performed at 30, 60, and 90 days as per ASTM C 1202–2019. The surface of the cylindrical disc layered with non-absorbent material were placed in the sample cell containing 3% of NaCl (-ve) and 0.3 N sodium hydroxide (+ve) solutions. A differential potential of 60 V was retained across the samples for 6 h, and the charge passed in coulombs was determined.

Experimental results

Properties of NFA and RFA

Table 3 shows the physical properties of NFA and FRA. From Table 1, it is observed that all the physical properties of FRA falls within the BIS limits excepting the water absorption. The water absorption of FRA was 86.9% more compared to NFA. This is due to the higher water absorption of FRA resulting from the adherence of mortar on the surface (Berredjem et al. 2020; Leite and Leite 2019; Khoshkenari et al. 2014). Figure 4 shows the grading curves of NFA and FRA. It is observed that the particle size of NFA and FRA was within the upper and lower bound limits of ASTM standards. Table 4 shows the chemical constituents of NFA and FRA. Figure 5 shows the XRD patterns of NFA and FRA. The peak in the pattern of NFA indicates the presence of crystalline mineral SiO_2. This could be favorable in the formation of C-S-H or C-A-S-H gel that promotes strength in the concrete. In case of FRA, the XRD pattern indicates the presence of two peaks of SiO_2 and $CaCO_3$. The presence of crystalline mineral SiO_2 clearly signifies the possibility of utilizing RFA as a suitable replacement to NFA. Also, the peak of $CaCO_3$ could be observed due to the adherence of cement mortar on the surface of FRA. Figure 6 shows the micro-structure of NFA and FRA. The SEM images show the sphericity of
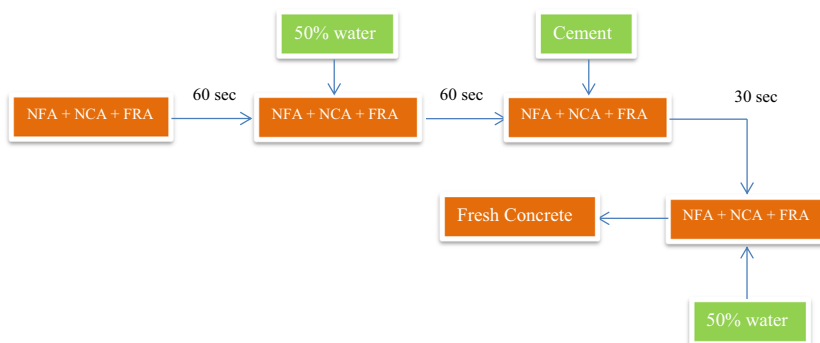
Fig. 3 Illustration of TSMA for concrete

Table 2 Mix proportions

Raw materials	(kg/m³)							
	R-0	R-25	R-50	R-100	MR-0	MR-25	MR-50	MR-100
Cement	400.00	413.00	413.00	413.00	400.00	413.00	413.00	413.00
NFA	799.00	599.25	399.5	0	799.00	599.25	399.5	0
RFA	0	199.75	399.5	799.00	0	199.75	399.5	799.00
20 mm NCA	617.40	617.40	617.40	617.40	617.40	617.40	617.40	617.40
10 mm NCA	411.60	411.60	411.60	411.60	411.60	411.60	411.60	411.60
Water	180.00	186.00	186.00	186.00	180.00	186.00	186.00	186.00
w/c ratio	0.45	0.45	0.45	0.45	0.45	0.45	0.45	0.45

NFA and angularity of FRA particles. The higher angularity of FRA was due to the crushing of concrete into finer fractions, and also the trace of adhered mortar on the surface of FRA was observed.

Workability

Figure 7 shows the workability of NAC, FRAC, and M-FRAC mixes. From Fig. 7, it is observed as the FRA increases, the slump of the concrete decreases (Kirthika and Singh 2020; Fan et al. 2016; Berredjem et al. 2020). The decrease in the slump of the concrete can be attributed to the rough texture and higher angularity of FRA particles as observed in Fig. 1. Also, adherence of mortar on the surface of FRA absorbs more water during mixing ultimately decreasing the slump of the concrete. The M-FRAC shows higher slump compared to the FRAC due to influence of TSMA. In TSMA, water was added in two stages, as the first stage results in the development of non-porous stiff matrix wrapping the surface of FRA particles and remaining water added during the second stage completes the process. The formation of non-porous mortar mix reduces the excess water absorption by FRA particles during mixing and hence resulting in higher slump of the concrete. The higher slump indicates the better workability of the concrete mixes.

Table 3 Physical properties of NFA and FRA

Properties	NFA	FRA	BIS limits (IS 383)
Specific gravity	2.58	2.42	2–3
Water absorption (%)	0.93	7.14	0.1–2
Bulk Density (kg/m³)	1528	1433	1200–1750
Fineness modulus	3.07	3.52	2.00–4.00
Silt content (%)	2.50	4.61	<8

Hardened properties

The influence of the FRA on the hardened properties of the NAC, FRAC, and M-FRAC mixes was evaluated by compressive strength, split tensile strength, and flexural strength. Table 5 shows the hardened properties of FRAC and M-FRAC at 7, 28, and 90 days.

Compressive strength

Figure 8 shows the compressive strength of the FRAC and M-FRAC mixes. From Fig. 8, it is observed that as FRA increases, the strength of the concrete decreases. The compressive strength of MR-25 is more compared to all other mixes. The strength of R-25 is 1.73% more compared to R-0 at 28 days and 3.95% more compared to R-0 at 90 days. However, the strength of R-50 is 6.62% less compared to R-0, and the strength of R-100 is 22.06% less compared to R-0 at 28 days. The decrease in the strength of FRAC is due to the higher porosity of FRA
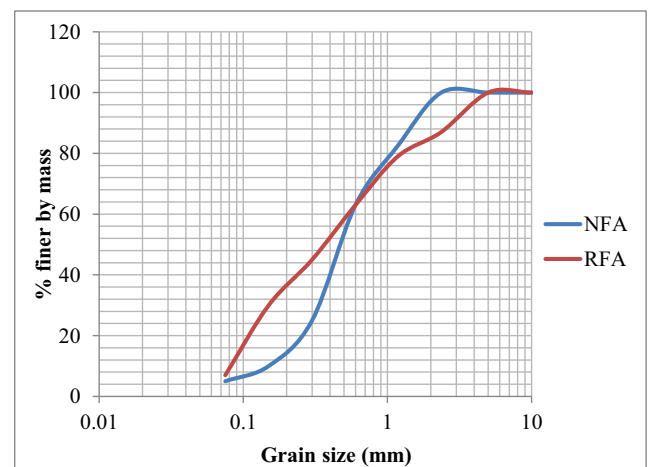

Fig. 4 Grading curves of NFA and FRA

Table 4 Chemical constituents of NFA and FRA

Compounds	NFA	FRA
SiO_2	90.24	71.24
Al_2O_3	2.31	5.51
Fe_2O_3	3.17	5.16
CaO	1.06	14.13
MgO	0.24	0.84
K_2O	1.31	1.03
Na_2O	1.27	0.67
Others	0.40	1.42

resulting from the adherence of mortar on its surface (Solyman 2005, Khatib 2005, Leite and Leite 2019). The strength of R-50 is 5.23% less compared to R-0, and the strength of R-100 is 19.53% less compared to R-0 at 90 days. It is observed that increased curing reduces the percentage decrease in the strength of the concrete (Berredjem et al. 2020; Kirthika and Singh 2020). As the curing period increases, better interconnectivity of pores results in the strength improvement of the concrete. When the concrete mixtures are prepared with TSMA, the strength of FRAC was further increased at 28 and 90 days. The strength of MR-25 is 4.04% more compared to MR-0 and 5.02% more compared to R-0 at 28 days. The strength of MR-50 is 5.92% less compared to MR-0 and 3.88% more compared to R-0. The strength of MR-100 is 20.27% less compared to MR-0 and 11.82% less compared to R-0. Furthermore, it is observed that TSMA increases the replacement level of FRA in the concrete. This is due to the improvement in the quality of ITZ through TSMA approach that enhanced the strength of the concrete (Liang et al. 2015, Tam et al. 2005, Tam and Tam 2008).

Split tensile strength

Figure 9 shows the split tensile strength of the FRAC and M-FRAC mixes. From Fig. 9, it is observed that the split tensile strength decreases as the FRA increases. The tensile strength of MR-25 is more compared to all other mixes. The tensile strength of R-25 is 1.10% more compared to R-0 at 28 days and 2.55% more compared to R-0 at 90 days. However, the strength of R-50 is 4.48% less compared to R-0, and the strength of R-100 is 15.41% less compared to R-0 at 28 days. This can be attributed to the increase in the pore volume and adherence of mortar on the surface of FRA that weakens the bond of cement matrix with FRA (Kirthika and Singh 2020). Similar trend of decrease in the strength reduction with increased curing was observed in split tensile strength also. The strength of R-50 is 3.57% less compared to R-0, and the strength of R-100 is 13.51% less compared to R-0 at 90 days. When the concrete mixtures are prepared with TSMA, the split tensile strength of FRAC was further increased at 28 and 90 days. The strength of MR-25 is 3.26% more compared to MR-0 and 14.28% more compared to R-0 at 28 days. The strength of MR-50 is 7.17% less compared to MR-0 and 4.54% more compared to R-0. The strength of MR-100 is 16.24% less compared to MR-0 and only 5.47% less compared to R-0 at 90 days. It is observed that the split tensile strength increases in the same trend of compressive strength but at a decreasing rate (Neville 2003).

Flexural strength

Figure 10 shows the flexural strength of the FRAC and M-FRAC mixes. From Fig. 10, it is observed that the flexural strength decreases as the FRA increases. The flexural strength of MR-25 is more compared to all other mixes. The flexural strength of R-25 is 0.68% more
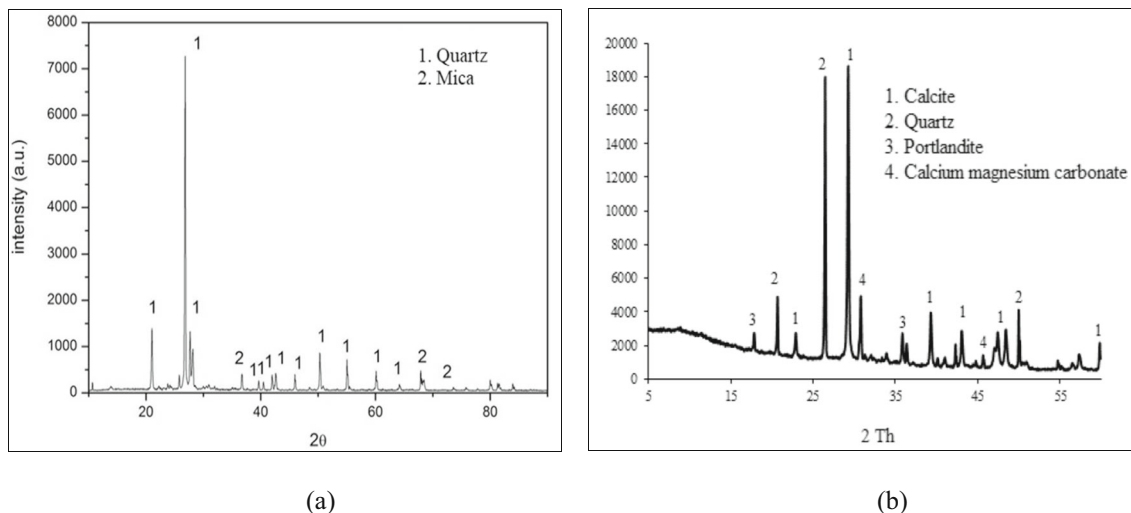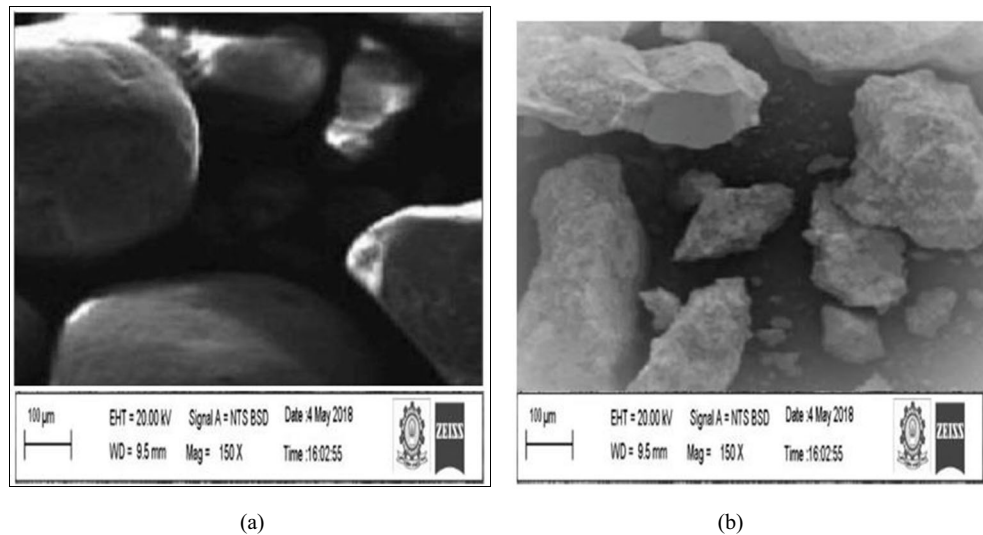

(a)

(b)

Fig. 5 XRD patterns of **a** NFA and **b** FRA

Fig. 6 SEM images of **a** NFA and **b** FRA

(a)   (b)

compared to R-0 at 28 days and 1.98% more compared to R-0 at 90 days. However, the strength of R-50 is 3.42% less compared to R-0, and the strength of R-100 is 11.87% less compared to R-0 at 28 days. This can be attributed to the high angularity of FRA and higher porosity resulting from the presence of adhered mortar (Li et al. 2019). Similar trend of decrease in the strength reduction with increase in the curing ages was also observed in flexural strength. The strength of R-50 is 2.63% less compared to R-0, and the strength of R-100 is 10.32% less compared to R-0 at 90 days. When the concrete mixtures are prepared with TSMA, the strength of FRAC was further increased at 28 and 90 days. The strength of MR-25 is 2.52% more compared to MR-0 and 14.06% more compared to R-0 at 28 days. The strength of MR-50 is 3.11% less compared to MR-0 and 11% more compared to R-0. The strength of MR-100 is 12.38% less compared to MR-0 and only 4.04% less compared to R-0 at 90 days.

Fig. 7 Workability of concrete mixes

Durability properties

The influence of the FRA on the durability of the NAC, FRAC, and M-FRAC mixes was evaluated by water absorption, porosity, sorptivity, shrinkage, and RCPT and carbonation tests. Table 6 shows the durability properties of NAC, FRAC, and M-FRAC mixes at the respective ages.

Water absorption and Porosity

Figure 11 shows the water absorption and porosity of FRAC and M-FRAC mixes. From Fig. 11, it is observed that as the FRA increases, the porosity increases and hence the water absorption of the concrete increases. All the mixes excepting R-25 and MR-25 show less water absorption and porosity compared to R-0. The water absorption and porosity of R-25 was 8.02% and 9.09% less compared to R-0 at 28 days. Similarly, the water absorption and porosity of MR-25 was 10% and 14.29% less compared to MR-0 at 28 days. It is observed that the maximum porosity of 0.17% was observed in R-100 with the maximum absorption of 6.73% at 28 days. The water absorption of R-50 and R-100 is 12.78% and 23.92% more compared to R-0 at 28 days. The porosity of R-50 and R-100 is 7.69% and 29.41% more compared to R-0 at 28 days. This can be attributed to the poor quality of FRA, higher void content resulting from the adherence of mortar on the surface of FRA (Levy and Helene 2007, Fumoto and Yamada 2002, Evangelista and de Brito 2010). Eventually, when the curing period increases, the porosity and water absorption of the concrete mixes was increased but at a minimum rate. The water absorption of R-0, R-25, R-50, and R-100 at 90 days is 2.29%, 1.86%, 2.65%, and 3.44% more compared to the similar mixes at 28 days. The porosity of R-0, R-25, R-50, and R-100 at 90 days is 20%, 15.38%, 18.75%, and 19.05% more compared to the similar mixes at
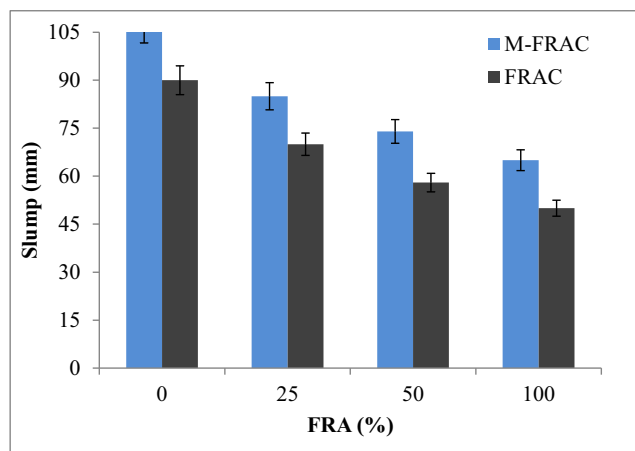
Table 5 Hardened properties of FRAC and M-FRAC mixes

Mix ID	Compressive strength (MPa)			Split tensile strength (MPa)			Flexural strength (MPa)		
	7 days	28 days	90 days	7 days	28 days	90 days	7 days	28 days	90 days
R-0	27.69	39.07	49.85	2.84	3.57	4.20	3.68	4.38	4.94
R-25	27.94	39.76	51.92	2.85	3.61	4.31	3.70	4.41	5.04
R-50	25.72	36.48	47.24	2.70	3.41	4.05	3.55	4.23	4.81
R-100	22.21	30.45	40.11	2.45	3.02	3.63	3.30	3.86	4.43
MR-0	30.62	43.21	59.75	3.03	3.82	4.74	3.87	4.60	5.41
MR-25	30.94	45.03	62.91	3.06	3.92	4.90	3.89	4.70	5.55
MR-50	28.32	40.65	53.43	2.88	3.66	4.40	3.73	4.46	5.12
MR-100	25.31	34.45	45.88	2.67	3.28	3.97	3.52	4.11	4.74

28 days. This can be attributed to the higher initial water absorption by FRA particles (Solyman 2005). When the concrete mixtures are prepared with TSMA, the water absorption and porosity of the M-FRAC mixes was further reduced. The water absorption of MR-0, MR-25, MR-50, and MR-100 at 90 days is only 1.75%, 1.34%, 1.99%, and 2.21% more compared to the same mixes at 28 days. Similarly, the porosity of MR-0, MR-25, MR-50, and MR-100 at 90 days is only 12%, 9.09%, 14.81%, and 16.67% more compared to the same mixes at 28 days.

Sorptivity

Figure 12 shows the sorptivity of FRAC and M-FRAC mixes. From Fig. 12, it is observed that as the FRA increases, the sorptivity increases with time. Also, the sorptivity increases rapidly in the first 30 min to 1 h and increases slowly beyond 1 until 5 h. This can be attributed to the extended capillaries resulting from higher porosity of FRAC that increased the uptake of water by the specimens due to capillary stress (Fan et al. 2016, Berredjem et al. 2020, Evangelista and de Brito 2010). For example, at the first 30 min, the capillary rise of R-25 was 2.21 g/mm^2, whereas the capillary rise at 5th hour

was only 4.75 g/mm^2. Similarly, the capillary rise of MR-25 at 30th minute was 1.61 g/mm^2 whereas the capillary rise at 5th hour was only 4.26 g/mm^2. The maximum capillary rise was observed with R-100 as 2.40 g/mm^2, and minimum capillary rise was observed with MR-0 as 1.76 g/mm^2 at 30th minute. It is observed that the M-FRAC specimens show less initial surface absorption compared to FRAC specimens even at identical replacement levels. The difference in the initial surface absorption is due to the refinement of porous network of FRA particles through TSMA approach that reduced the void content in the concrete mixtures. Even though the presence of FRA particles increases the capillary rise of concrete mixes, addition of mineral admixtures might refine the pore structure of FRAC and reduce the sorptivity. This was evident through the findings of (Sim and Park 2011, Mindess et al. 2002) where the permeability of concrete was reduced with addition of supplementary cementitious materials.

Shrinkage

Figure 13 shows the shrinkage of FRAC and M-FRAC mixes. From Fig. 13, it is observed that as the FRA increases, the
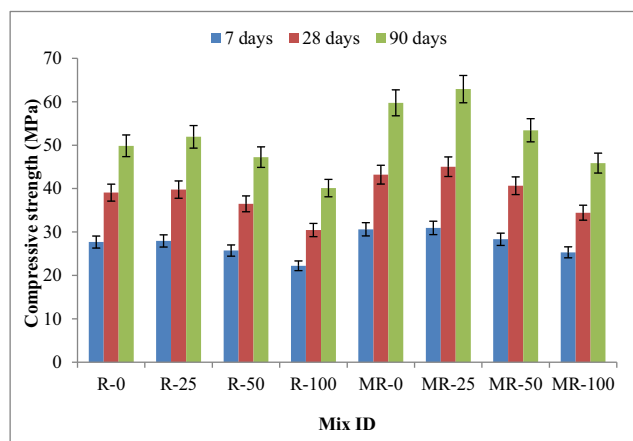
Fig. 8 Compressive strength of FRAC and M-FRAC
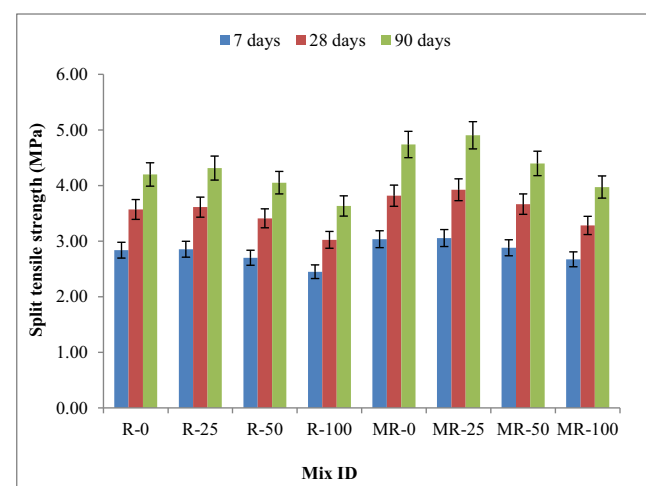
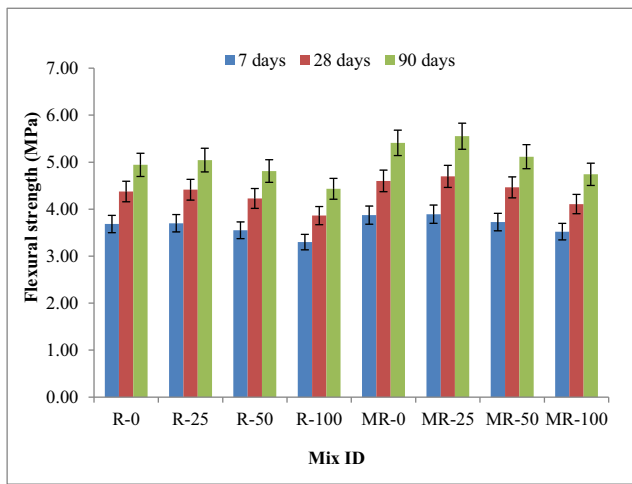**Fig. 9** Split tensile strength of FRAC and M-FRAC

Fig. 10 Flexural strength of FRAC and M-FRAC

drying shrinkage increases for both FRAC and M-FRAC mixes. It is observed that excepting R-25 and MR-25, all other FRAC mixes shows higher drying shrinkage compared to R-0. The increase in the drying shrinkage can be attributed to (i) poor quality of FRA particles that reduces the volumetric stability of FRAC mixes, (ii) presence of excess fine dust and un-hydrated cement particles on the FRA that absorbs more water, and (iii) high angularity of FRA particles leading to increase in the water content. The obtained results are similar to the findings of Kirthika and Singh (2020), Li et al. (2019), and Khatib (2005). The above factors increase the porosity of the concrete mixes and thereby increasing the drying shrinkage. Conversely, the mix MR-25 shows still lesser shrinkage values compared to R-25. However, the shrinkage of MR-100 was found to be 12.24% more compared to MR-0 whereas the shrinkage of R-100 was 17% more compared to R-0 at 28 days. This is due to the densification of pore structure and ITZ through TSMA approach that reduced the shrinkage of M-FRAC mixes. In addition, it is observed that increased curing decreases the shrinkage of FRAC and M-FRAC mixes.

The rate of increase in the shrinkage of R-100 at 56 days was 10%, whereas it was only around 7% at 90 days. Similar results are also observed in case of M-FRAC mixes at higher curing ages.

Rapid chloride penetration (RCPT)

Figure 14 shows the RCPT for FRAC and M-FRAC mixes. From Fig. 16, it is observed that the total charge passed is higher for all mixes excepting R-25 and MR-25. This can be attributed to the higher porosity of the concrete mixes resulting from the adherence of mortar (Evangelista and de Brito 2010, Sim and Park 2011). Various factors like excess free water content, presence of adhered mortar, and weak ITZ contribute to the increase in the porosity of the FRAC mixes. As the porosity of the concrete mixture increases, the rate of chloride ion penetration into the concrete mixture increases and hence affecting the integrity of the micro-structure. Conversely, increased curing period decreases the chloride ion penetration irrespective of the replacement levels (Sim and Park 2011; Kirthika and Singh 2020). The charge passed in coulombs for R-100 at 30 days was found to be 4200 C, whereas at 60 days it is found to be 3750 C. This can be attributed to the densification of micro-structure of the concrete and hence improving the resistance of FRAC and M-FRAC mixes to the chloride ion penetration. Furthermore, the resistance of M-FRAC mixes was better compared to FRAC as it is evident that the penetration rate of MR-100 was 9.52% lesser compared to R-100, respectively.
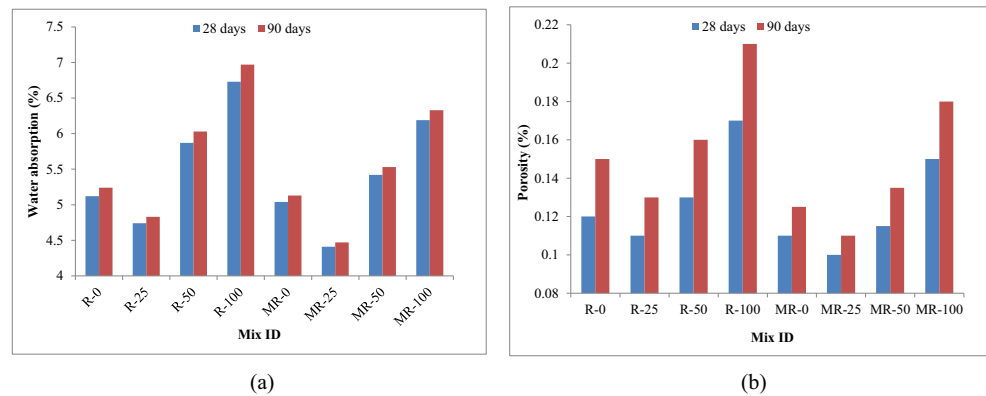
Carbonation

Figure 15 shows the depth of carbonation and carbonation coefficient of FRAC and M-FRAC mixes. The rate of carbonation of FRAC and M-FRAC is shown in Fig. 16. The depth of carbonation increases with increase in the FRA replacement

Table 6 Durability properties of FRAC and M-FRAC mixes

Mix ID	Water absorption (%)		Porosity (%)		Shrinkage ($\times 10^{-6}$)				RCPT (coulombs)		Carbonation depth (mm)		
	28 days	90 days	28 days	90 days	7 days	28 days	56 days	90 days	30 days	60 days	30 days	60 days	90 days
R-0	5.12	5.24	0.12	0.15	180	365	420	462	2200	1500	6.57	13.69	20.27
R-25	4.74	4.83	0.11	0.13	174	327	357	380	1700	1100	7.67	14.79	21.91
R-50	5.87	6.03	0.13	0.16	181	394	434	471	2600	1900	8.49	15.88	24.10
R-100	6.73	6.97	0.17	0.21	203	438	483	525	4200	3750	9.86	18.07	27.93
MR-0	5.04	5.13	0.11	0.125	175	324	378	397	2100	1450	5.48	11.50	17.53
MR-25	4.41	4.47	0.1	0.11	159	284	306	317	1550	900	6.02	12.60	18.62
MR-50	5.42	5.53	0.115	0.135	177	366	408	427	2400	1800	7.12	14.79	20.27
MR-100	6.19	6.33	0.15	0.18	194	392	428	461	3800	3600	8.22	16.43	21.91

Fig. 11 **a** Water absorption and **b** porosity

(a)

(b)

excepting for R-25 and MR-25. The increase in the depth of carbonation upon increase in the replacement of FRA can be attributed to the increase in the void content of the mixes as a result of increased porosity. This paves way for the entry of CO_2 into the concrete and hence affecting the micro-structure of the concrete. The depth of carbonation of R-100 was 21.55% more compared to R-0, and the depth of carbonation of MR-100 was 15.01% more compared to MR-0 at 90 days. When the concrete mixtures are prepared with TSMA, the internal structure of the concrete was densified with less voids and hence hindering the entry of CO_2 into the concrete. Similar other studies performed by Kirthika and Singh (2020), Evangelista et al. (2010), Zega and Di Maio (2011) infer that as the FRA increases, the carbonation of the concrete increases.

Discussions

This research study involves the investigation on the utilization of FRA on the hardened and durability properties of the concrete. Previous studies performed by Solyman (2005), Khatib (2005), and Evangelista et al. (2010) inferred that the quality of FRA was poor compared to NFA due to the presence of fine dust particles and adhered mortar. In this study,
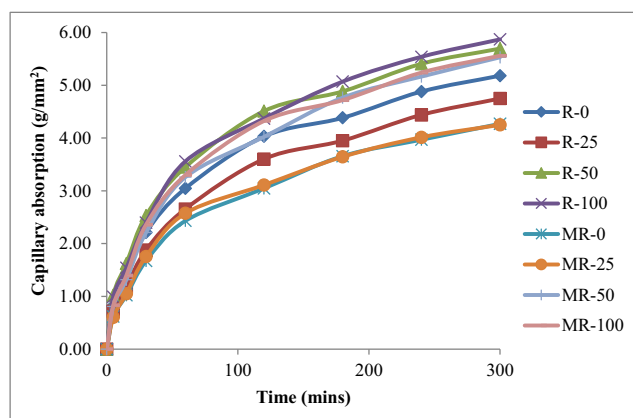
the FRA particles were pre-saturated to achieve SSD before mixing in the concrete. The FRA particles examined for its physical properties show inferior results compared to NFA. However, all the properties of FRA falls within the BIS limits excepting the water absorption (Li et al. 2019, Pereira et al. 2012, Ju et al. 2019).

To counteract the effect of poor quality of FRA that affects the properties of the concrete, the concrete mixtures are prepared with TSMA technique. In TSMA, the water is added in two stages in such a way that excess water absorption by FRA affecting the water requirement for hydration was detained (Tam et al. 2005; Tam and Tam 2008; Liang et al. 2015). The effect of TSMA on the fresh, hardened, and durability properties of M-FRAC mixes was evaluated and compared with FRAC mixes. Increase in the replacement of FRA decreases the slump of the concrete (Geng and Sun 2013; Braga et al. 2012), but the slump was increased with M-FRAC mixes even at identical replacement levels. This is because the porous FRA was wrapped with non-porous stiff matrix exempting the excess absorption of mixing water by FRA and hence improving the workability of the concrete.

The hardened properties of the FRAC and M-FRAC were evaluated by compressive strength, split tensile
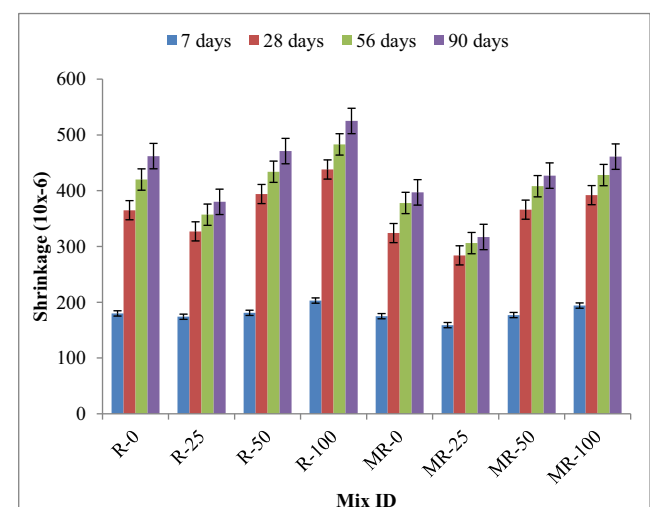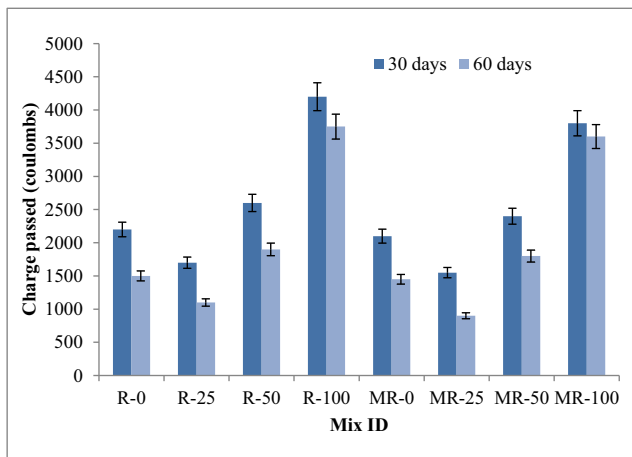

Fig. 12 Sorptivity of FRAC and M-FRAC

Fig. 13 Shrinkage of FRAC and M-FRAC mixes

Fig. 14 RCPT for FRAC and M-FRAC

properties of the concrete. Also, it is observed that the voids and cracks in the ITZ of FRAC is large compared to that of NAC as a result of which less water for hydration was available at the ITZ of FRAC. Concerning to durability properties, higher water absorption of FRA resulted in the higher porosity of the FRAC mixes. As a result of the high porosity, other successive durability parameters such as water absorption, sorptivity, chloride penetration, carbonation, and shrinkage of FRAC was more compared to NAC. When cured at higher ages, better interconnectivity of pores resulted in the enhancement of the durability properties of FRAC. Improvement in the durability properties of M-FRAC through TSMA was observed but less compared to that of NAC. Densification of the micro-structure through TSMA will reduce the pore volume in the concrete and hence improves the durability properties of M-FRAC. Similar trend of improvement in the durability properties of M-FRAC at increased curing was observed.

strength, and flexural strength. Increase in the replacement beyond 25% decreases the strength of both FRAC and M-FRAC mixes. This can be attributed to the weak ITZ resulting from the high porosity of FRA. As we know, the ITZ decides the strength of the concrete; modification to the internal micro-structure through TSMA will improve the strength of ITZ. The FRAC concrete comprises of two ITZ with one between the FRA and new cement mortar and other between the old mortar and new mortar. The latter ITZ is the weakest link, and hence, modification by TSMA will produce non-porous stiff matrix that clog the micro-cracks in the ITZ of the FRAC. This in turn will improve the ITZ, and hence, better strength and durability properties were observed in M-FRAC mixes compared to FRAC mixes. Figure 17 shows the micro-structure of NAC, FRAC, and M-FRAC mixes. From Fig. 17, it is observed that the micro-structure of FRAC possesses voids with micro-cracks on the ITZ. In case of M-FRAC, a non-porous stiff matrix prepared by TSMA clogs the micro-pores and densifies the ITZ of the FRAC. Improvement in the quality of ITZ will eventually improve the strength and durability

Conclusion

The influence of FRA on the strength and durability of the FRAC and M-FRAC was investigated and compared with NAC. The properties of FRAC were affected by the higher water absorption of FRA resulting from the adherence of mortar. Hence, the concrete mixtures are prepared with TSMA and evaluated for its fresh, hardened, and durability properties and compared with FRAC and NAC. The following conclusions are drawn as follows:

1. The water absorption of FRA is 86.9% more compared to NFA that affects the properties of the concrete.
2. The fresh and hardened properties of FRAC decrease with an increase in the replacement of FRA beyond 25%. MR-25 shows 5.02%, 3.26%, and 2.52% increase in the compressive strength, split tensile strength, and flexural strength compared to MR-0 at 90 days. However, the
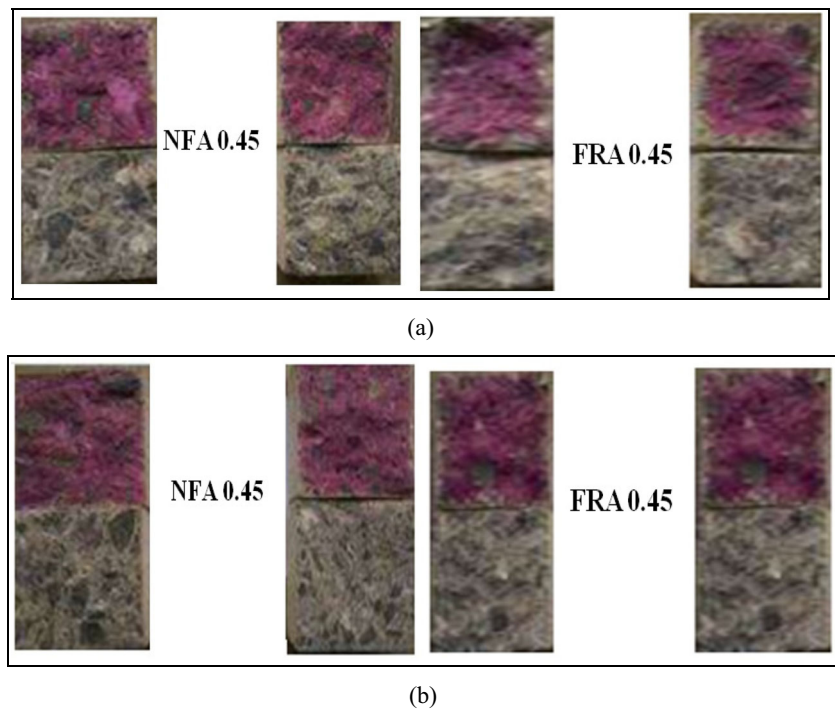
Fig. 15 a Carbonation depth and **b** carbonation coefficient
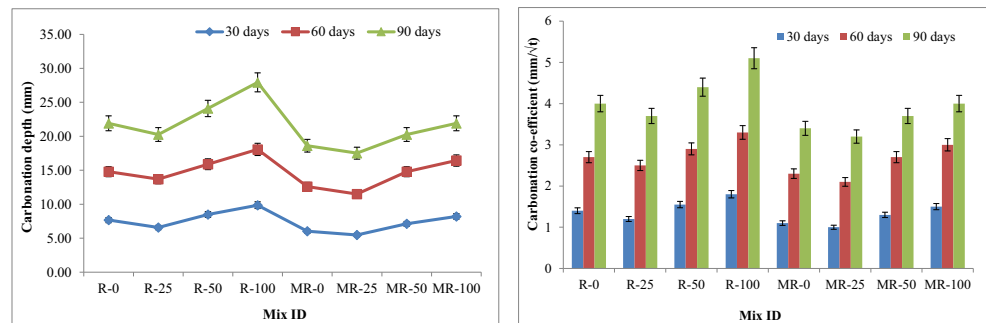
(a)

(b)

Fig. 16 Rate of carbonation of **a** FRAC and **b** M-FRAC

(a)

(b)

fresh and hardened properties of M-50 were nearly comparable to that of R-25 at 28 and 90 days and hence increasing the replacement levels of FRA.

3. Higher water absorption of FRA increased the porosity of the concrete. The pore volume of R-0 and R-100 was 0.21% and 0.15% at 90 days. Similarly the pore volume

Fig. 17 Micro-structure of **a** NAC, **b** FRAC, and **c** M-FRAC

(a)

(b)

(c)
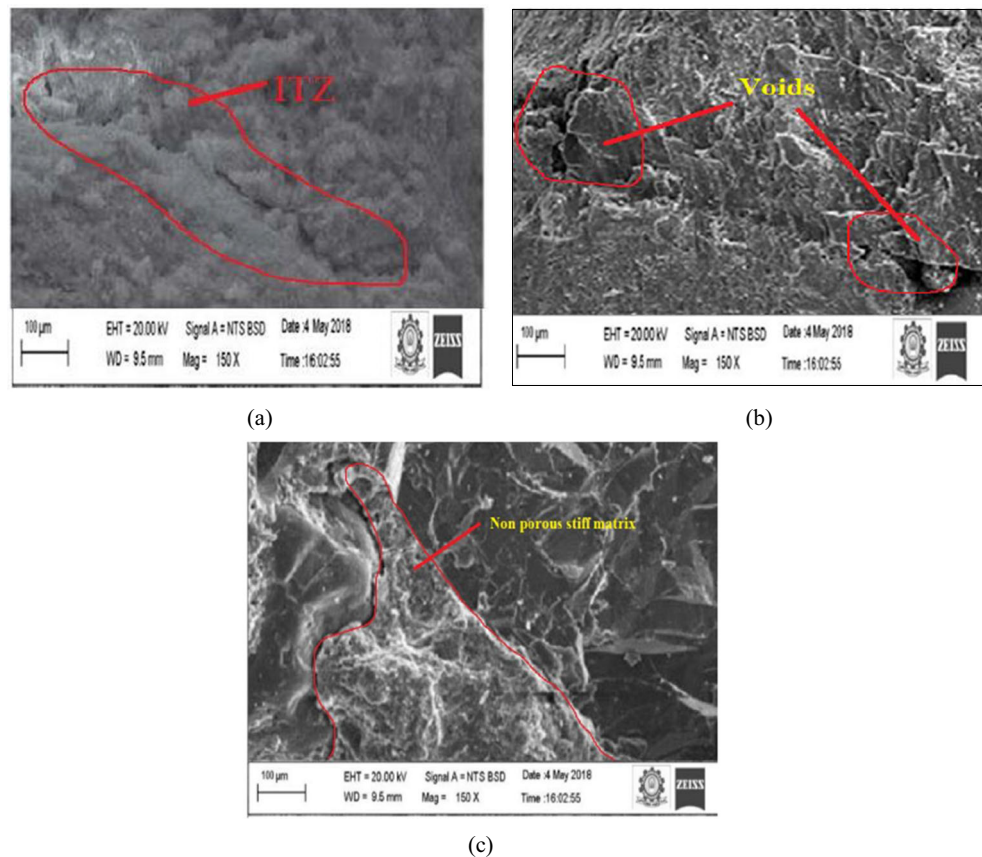
of MR-100 and MR-0 was 0.18% and 0.125% at 90 days, respectively. The higher porosity of FRAC eventually increases the water absorption of R-100 to 6.97% and R-0 to 5.24% at 90 days.

4. The sorptivity increases rapidly in the first 30 min to 1 h and increases slowly beyond 1 until 5 h due to the extended capillaries resulting from higher absorption of FRA.

5. The shrinkage of R-25 was found to be 17.74% less compared to R-0 and the shrinkage of MR-25 was found to be 20.15% less compared to MR-0 at 90 days.

6. Owing to high pore volume, the rate of chloride ingression of R-100 and MR-100 was higher compared to R-0. The charge passed in R-100 were 47.6% more compared to R-0, whereas the charge passed in MR-100 was 44% more compared to R-0 at 30 days.

7. The presence of excess void content increased the rate of CO_2 penetration in FRAC mixes. The depth of carbonation for R-100 was 21.55% more compared to R-0, and depth of carbonation for MR-100 was 15.01% more compared to MR-0 at 90 days.

The research provides an outcome on understanding the feasibility of utilization of FRA as a suitable replacement to NFA in the concrete and improvement in the properties of FRAC through TSMA. The findings of the research infer that 25% replacement of FRA will improve the hardened and durability properties of the concrete. Also, increased curing improves the strength and durability properties of FRAC that is comparable to NAC. Also, the concrete mixes prepared with TSMA exhibits densified micro-structure that improved the strength and durability properties compared to NMA. Further studies on the utilization of supplementary cementitious materials may increase the replacement levels of FRA in the concrete with better strength and durability properties.

Declarations

References

Abrahams M, Rakesh R (2018) Manufacturing Concrete with high compressive strength using recycled aggregates. J Mater Civ Eng 30(8): 04018182. https://doi.org/10.1061/(ASCE)MT.1943-5533. 0002398

ASTM C1202-19 (2019) Standard Test Method for Electrical Indication of Concrete's Ability to Resist Chloride Ion Penetration. ASTM International, West Conshohocken. https://www.astm.org. Accessed Oct to Nov 2020

ASTM C1585-20 (2020) Standard Test Method for Measurement of Rate of Absorption of Water by Hydraulic-Cement Concretes. ASTM International, West Conshohocken. https://www.astm.org. Accessed Oct to Nov 2020

ASTM C39 / C39M-20 (2020) Standard Test Method for Compressive Strength of Cylindrical Concrete Specimens. ASTM International, West Conshohocken. https://www.astm.org. Accessed Oct to Nov 2020

ASTM C596. 2018 (2020) Standard Test Method for Drying Shrinkage of Mortar Containing Hydraulic Cement. Annual Book of ASTM Standards. ASTM, International, West Conshohocken. https://www.astm.org. Accessed Oct to Nov 2020

ASTM C78 / C78M-18 (2018) Standard Test Method for Flexural Strength of Concrete. ASTM International, West Conshohocken. https://www.astm.org. Accessed Oct to Nov 2020

Berredjem L, Arabi L, Molez L (2020) Mechanical and durability properties of concrete based on recycled coarse and fine aggregates produced from demolished concrete. Constr Build Mater 246:118421. https://doi.org/10.1016/j.conbuildmat.2020.118421

Braga M, De Brito J, Veigo R (2012) Incorporation of fine concrete aggregates in mortars. Constr Build Mater 36:960–968. https://doi.org/10.1016/j.conbuildmat.2012.06.031

BS: 1881-208 (1996) Testing concrete. Recommendations for the determination of the initial surface absorption of concrete. British standards, London

Evangelista L, de Brito J (2010) Durability performance of concrete made with fine recycled concrete aggregates. Cem Concr Compos 32:9–14

Fan CC, Huang R, Hwang H, Chao SJ (2016) Properties of concrete incorporating fine recycled aggregates from crushed concrete wastes. Constr Build Mater 112:708–715. https://doi.org/10.1016/j.conbuildmat.2016.02.154

Fumoto T, Yamada M (2002) Influence of the quality of recycled fine aggregate on properties of concrete. Memoris of Faculty of Engineering (Symposium paper) 43:97–103 Osaka: Osaka City University

Geng J, Sun J (2013) Characteristics of the carbonation resistance of recycled fine aggregate concrete. Constr Build Mater 49:814–820

Ho NY, Yang PKL, Wee FL, Tarek Z, Keat CC, Giau LL, Seng KT (2013) Efficient utilization of recycled concrete aggregate in structural concrete. J Mater Civ Eng 25:318–327

IS 4031, Part 2-8 (1988) Methods of physical tests for hydraulic cement. Bureau of Indian Standards, New Delhi, India

IS: 10262 (2009) Guidelines for concrete mix design proportioning. Bureau of Indian Standards, New Delhi

IS: 1199 (1999) Methods of sampling and analysis of concrete. Bureau of Indian Standards, New Delhi

Ju M, Park K, Park W-J (2019) Mechanical Behavior of Recycled Fine Aggregate Concrete with High Slump Property in Normal- and High-Strength. International Journal of Concrete Structures and Materials 13

Katz A (2004) Treatments for the improvement of recycled aggregate. J Mater Civ Eng 16(6):597–603. https://doi.org/10.1061/(ASCE) 0899-1561(2004)16:6(597)

Khatib JM (2005) Properties of concrete incorporating fine recycled aggregates. Cem Concr Res 35:763–769

Khoshkenari AG, Shafigh P, Moghimi M, Mahmud HB (2014) The role of 0–2 mm fine recycled concrete aggregate on the compressive and splitting tensile strengths of recycled concrete aggregate concrete. Mater Des 64:345–354. https://doi.org/10.1016/j.matdes.2014.07.048

Kirthika SK, Singh SK (2020) Durability studies on recycled fine aggregate concrete. Constr Build Mater 250:118850. https://doi.org/10.1016/j.conbuildmat.2020.118850

Leite MM, Leite VM (2019) Evaluation of an experimental mix proportion study and production of concrete using fine recycled aggregate. Journal of Building Engineering 21:243–253. https://doi.org/10.1016/j.jobe.2018.10.016

Levy S, Helene P (2007) Durability of concrete mixed with fine recycled aggregates. Exacta 5:25–34

Li L, Zhan BJ, Lu J, Poon CS (2019) Systematic evaluation of the effect of replacing river sand by different particle size ranges of fine recycled concrete aggregates (FRCA) in cement mortars. Constr Build Mater 209:147–155

Liang YC, Ye ZM, Vernerey F, Xi Y (2015) Development of processing methods to improve strength of concrete with 100% recycled coarse aggregate. J Mater Civ Eng 27(5):04014163. https://doi.org/10.1061/(ASCE)MT.1943-5533.0000909

Mindess S, Young JF, Darwin D (2002) Concrete, second edn. Prentice Hall, New Jersey

Neville AM (2003) Properties of Concrete, 5th edn. Pearson Education Limited, London

Otsuki N, Miyazato SI, Yodsudjai W (2003) Influence of recycled aggregate on interfacial transition zone, strength, chloride penetration and carbonation of concrete. J Mater Civ Eng 15:443–451

Pereira P, Evangelista L, de Brito J (2012) The effect of superplasticizers on the mechanical performance of concrete made with fine recycled concrete aggregates. Cem Concr Compos 34:1044–1052

Poon CS, Shui ZH, Lam L, Fok H, Kou SC (2004) Influence of moisture states of natural and recycled aggregates on the slump and compressive strength of concrete. Cem Concr Res 34:31–36

Revathi P, Amirthavalli RR, Lavanya K (2014) Influence of treatment methods on the strength and performance characteristics of recycled aggregate concrete. J Mater Civ Eng 27(5):04014168. https://doi.org/10.1061/(ASCE)MT.1943-5533.0001128

Saravanakumar P, Abhiram K, Manoj B (2016) Properties of treated recycled aggregates and its influence on concrete strength characteristics. Constr Build Mater 111:611–617. https://doi.org/10.1016/j.conbuildmat.2016.02.064

Sim J, Park C (2011) Compressive strength and resistance to chloride ion penetration and carbonation of recycled aggregate concrete with varying amount of fly ash and fine recycled aggregate. Waste Manag 31:2352–2360. https://doi.org/10.10016/j.wasman.2011.06.014

Solyman M (2005) Classification of recycled sands and their applications as fine aggregates for concrete and bituminous mixtures (Unpublished PhD thesis). Fachbereich Bauingenieurwesen der Universität Kassel, Kassel, Germany, 196 p

Tam VWY, Tam CM (2008) Diversifying two-stage mixing approach (TSMA) for recycled aggregate concrete: TSMAs and TSMAsc. Constr Build Mater 22(10):2068–2077. https://doi.org/10.1016/j.conbuildmat.2007.07.024

Tam VW, Gao XF, Tam CM (2005) Micro-structural analysis of recycled aggregate concrete produced from two-stage mixing approach. Cem Concr Res 35(6):1195–1203. https://doi.org/10.1016/j.cemconres.2004.10.025

Vivian WYT, Soomro M, Evangelista ACJ (2018) A review of recycled aggregate in concrete applications (2000–2017). Constr Build Mater 172:272–292

Zega CJ, Di Maio AA (2011) Use of recycled fine aggregate in concretes with durable requirements. Waste Manag 31:2336–2340

Publisher's note Springer Nature remains neutral with regard to jurisdictional claims in published maps and institutional affiliations.